

## Magnetic and transport properties of Co-doped Fe<sub>3</sub>O<sub>4</sub> films

D. Tripathy and A. O. Adeyeye<sup>a)</sup>

*Information Storage Materials Laboratory, Department of Electrical and Computer Engineering, National University of Singapore, Singapore 117576, Singapore*

C. B. Boothroyd

*Institute of Materials Research and Engineering, 3 Research Link, Singapore 117602, Singapore*

S. N. Piramanayagam

*Data Storage Institute, DSI Building, 5 Engineering Drive 1, Singapore 117608, Singapore*

(Received 27 June 2006; accepted 21 October 2006; published online 8 January 2007)

We present a systematic study of the structural, magnetic, and magnetotransport properties of Co-doped Fe<sub>3</sub>O<sub>4</sub> films deposited on MgO (100) substrates by cosputtering technique. Transmission electron microscopy images suggest that the undoped and Co-doped Fe<sub>3</sub>O<sub>4</sub> films are polycrystalline in nature and consist of a well defined grain boundary network. The temperature dependence of resistance also shows that the transport mechanism in our films is dominated by electron tunneling across antiferromagnetically coupled grain boundaries. We observed that the magnetic properties of the doped films are markedly sensitive to the Co doping concentration, with the magnetization curves showing drastic changes in coercivity with increasing doping concentration. In-plane magnetoresistance curves show linear magnetic field dependence for the undoped Fe<sub>3</sub>O<sub>4</sub> films while a reduction in magnetoresistance and a departure from linear field dependence are observed for the Co-doped films. © 2007 American Institute of Physics. [DOI: 10.1063/1.2404469]

### I. INTRODUCTION

The magnetic and transport properties of half metallic Fe<sub>3</sub>O<sub>4</sub> films<sup>1-5</sup> have been extensively studied due to its high Curie temperature of 860 K and a predicted negative spin polarization of 100% by band structure calculations using local spin density approximation (LSDA) and self-consistent augmented plane wave (APW) methods.<sup>6,7</sup> Fe<sub>3</sub>O<sub>4</sub> is a ferrimagnet with a cubic inverse spinel structure, in which iron cations occupy the interstitial sites of a face centered cubic (fcc) closed packed frame of oxygen anions. Two kinds of cation sites exist in the crystal; A sites are tetrahedrally coordinated to oxygen and are occupied only by Fe<sup>3+</sup> ions, while B sites are octahedrally coordinated to oxygen and are occupied by an equal number of Fe<sup>2+</sup> and Fe<sup>3+</sup> ions.<sup>8</sup> A possible explanation for the observed ferrimagnetism in Fe<sub>3</sub>O<sub>4</sub> is the double exchange interaction through Fe<sup>2+</sup> and Fe<sup>3+</sup> ions at the B sites, while the A and B site spins are antiferromagnetically (AF) coupled. At room temperature, the high electronic conductivity of Fe<sub>3</sub>O<sub>4</sub> is attributed to rapid electron hopping between the Fe<sup>2+</sup> and Fe<sup>3+</sup> ions occupying the B sites.

Recently, research has focused on modifying the composition of Fe<sub>3</sub>O<sub>4</sub> by doping, so as to study its effect on the structural, magnetic, and transport properties. It has been reported that ions such as Mn<sup>2+</sup> and Zn<sup>2+</sup> have a preference to occupy the A sites, while Ni<sup>2+</sup> and Co<sup>2+</sup> ions tend to occupy the octahedral B sites in the inverse spinel structure.<sup>9</sup> Ishikawa *et al.*<sup>10</sup> have successfully prepared epitaxial films of Mn-doped magnetite (Mn<sub>x</sub>Fe<sub>3-x</sub>O<sub>4</sub>) using pulsed laser deposition technique and have confirmed that the doped films are

thermodynamically more stable than undoped Fe<sub>3</sub>O<sub>4</sub> films. They also observed that as Mn concentration in the doped film was increased, carrier concentration became lower, thus indicating potential for field effect transistor (FET) or magnetization reversal by spin injection. In another study, Lie *et al.*<sup>11</sup> have investigated the effect of Zn doping on the magnetoresistance (MR) of sintered Fe<sub>3</sub>O<sub>4</sub> ferrite and have demonstrated a maximum MR ratio of 7% for small amounts of doping. Chou *et al.*,<sup>12</sup> have investigated the magnetic and electron transport properties of Ni-doped Fe<sub>3</sub>O<sub>4</sub> ferrites which were prepared by mixing Fe<sub>3</sub>O<sub>4</sub> powder with NiO powder, followed by compressing into pellets and sintering in Ar atmosphere. They observed that the MR value of bulk Fe<sub>3</sub>O<sub>4</sub> can be enhanced by Ni doping, and the MR effect is mainly due to spin-dependent tunneling of electrons through insulating barriers. Doping Fe<sub>3</sub>O<sub>4</sub> with Co<sup>2+</sup> ions, however, presents an extremely interesting study due to the high magnetic anisotropy of Co and its corresponding effects on the inherent properties of Fe<sub>3</sub>O<sub>4</sub> films. In fact, the investigation of Co<sub>x</sub>Fe<sub>3-x</sub>O<sub>4</sub> ferrites became the prototype for understanding the large anisotropy of Co atoms in a spinel structure and the role of directional ordering in induced anisotropy.<sup>13</sup> Moreover, such ferrite films have also been used to provide unidirectional exchange biasing to soft films.<sup>14</sup> Thus, a systematic study of the effects of Co doping on Fe<sub>3</sub>O<sub>4</sub> films is of interest both from a fundamental viewpoint and also due to potential for applications.

In this work, we have used a simple cosputtering technique at room temperature to grow Co-doped Fe<sub>3</sub>O<sub>4</sub> films on MgO (100) substrates. We have carried out a detailed study of the effects of varying Co content on the structural properties and temperature-dependent magnetic and MR properties of Fe<sub>3</sub>O<sub>4</sub> films. We observed that the Co-doped films are

<sup>a)</sup>Author to whom correspondence should be addressed; electronic mail: eleaao@nus.edu.sg

polycrystalline and have an inverse spinel structure. The presence of well defined grain boundaries was confirmed in the Co-doped films using transmission electron microscopy. We observed that the Verwey transition does not appear for our films and that the tunneling of electrons across AF coupled grain boundaries dominates the transport properties of the films. We also observed that the structural, magnetic, and MR behavior of the doped films are markedly sensitive to the Co doping concentration.

## II. EXPERIMENTAL DETAILS

The Co-doped  $\text{Fe}_3\text{O}_4$  films were grown on MgO (100) substrates by cosputtering  $\text{Fe}_3\text{O}_4$  and Co targets at room temperature in a process pressure of  $5 \times 10^{-3}$  Torr. The base pressure of the chamber was better than  $3 \times 10^{-8}$  Torr before deposition. The MgO substrates were ultrasonically cleaned in acetone and alcohol for 15 min and rinsed in de-ionized (DI) water prior to deposition. The rf power supply for the  $\text{Fe}_3\text{O}_4$  target was kept constant, while the dc power of the Co target was varied so as to have different Co doping concentrations. The thickness of the films was kept at  $\sim 50$  nm. Microstructures of the doped  $\text{Fe}_3\text{O}_4$  films were examined by transmission electron microscopy (TEM). Phase identification and crystal structures of the doped films were characterized by conventional  $\theta$ - $2\theta$  x-ray diffraction (XRD) scans using  $\text{Cu } K_\alpha$  radiation. The magnetic properties of the  $\text{Fe}_3\text{O}_4$  films were characterized using a vibrating sample magnetometer (VSM). Electrical contacts to the films were made using standard optical lithography, metallization of 200 nm Al, followed by lift-off in acetone. The magnetotransport properties of the doped films were measured as a function of temperature in the standard four probe configuration.

## III. RESULTS AND DISCUSSION

### A. Structural characterization

We have carried out systematic XRD measurements in order to investigate the effect of Co doping on the crystal structure of the films. Shown in Fig. 1 are the representative  $\theta$ - $2\theta$  XRD scans of the doped  $\text{Fe}_3\text{O}_4$  films, as a function of Co doping concentration. From the XRD patterns, we observed that all peaks in both the undoped and Co-doped  $\text{Fe}_3\text{O}_4$  films can be assigned to the inverse cubic spinel structure of  $\text{Fe}_3\text{O}_4$ . This indicates that the crystal structure of the Co-doped films is similar to that of  $\text{Fe}_3\text{O}_4$ . It has been suggested that the XRD pattern of  $\text{Co}_x\text{Fe}_{3-x}\text{O}_4$  ( $0 \leq x \leq 0.3$ ) is experimentally indistinguishable from that of  $\text{Fe}_3\text{O}_4$  and  $\text{CoFe}_2\text{O}_4$ .<sup>15</sup> Moreover, we did not detect any crystal orientation corresponding to Co in the doped films. This observation indicates further that Co ions possibly substitute Fe ions in the inverse spinel structure of  $\text{Fe}_3\text{O}_4$  to form a polycrystalline Co ferrite. It should also be noted that the strongest peak in our samples is (400) followed by (222). This indicates that the films have a preferred growth direction as compared to a truly random crystalline orientation which results in the strongest peak as (311) followed by (440) and (220). Interestingly, we also observed that the relative intensity of the (222) to the (400) peak increases as we increase the Co doping concentration. This may be attributed to the fact that

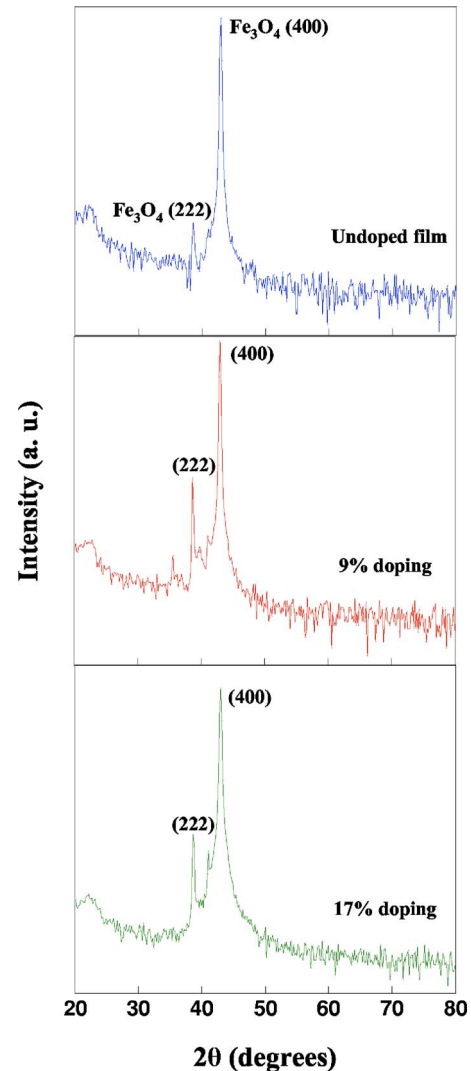


FIG. 1. (Color online) XRD patterns for Co-doped  $\text{Fe}_3\text{O}_4$  films as a function of Co doping concentration.

incorporation of Co in the inverse spinel structure of  $\text{Fe}_3\text{O}_4$  enhances the Co/Fe ratio in the films, which leads to a modification of the preferred growth direction and structural anisotropy of the doped films.

We have studied the microstructure of the undoped and 17% Co-doped  $\text{Fe}_3\text{O}_4$  films. Figure 2(a) shows the high resolution bright field TEM image for the undoped  $\text{Fe}_3\text{O}_4$  film. We observed well defined grains with a mean grain size of about 12 nm. Another noticeable feature in the image is the presence of a large density of grain boundaries separating the grains. For the 17% Co-doped  $\text{Fe}_3\text{O}_4$  film [Fig. 2(b)], the grain boundary network is still existent, while the mean grain size decreases. These grain boundaries have uniform width and a consistent contrast which may be attributed to the presence of an amorphous Fe-oxide phase at the boundary.<sup>16</sup> Shown in Fig. 2(c) is the selected area electron diffraction (SAED) pattern for the 17% Co-doped  $\text{Fe}_3\text{O}_4$  film. The bright spots in the diffraction pattern come from the MgO substrate, while the rings indicate that the Co-doped film is polycrystalline in nature. We detected no diffraction rings from Co in the doped films.

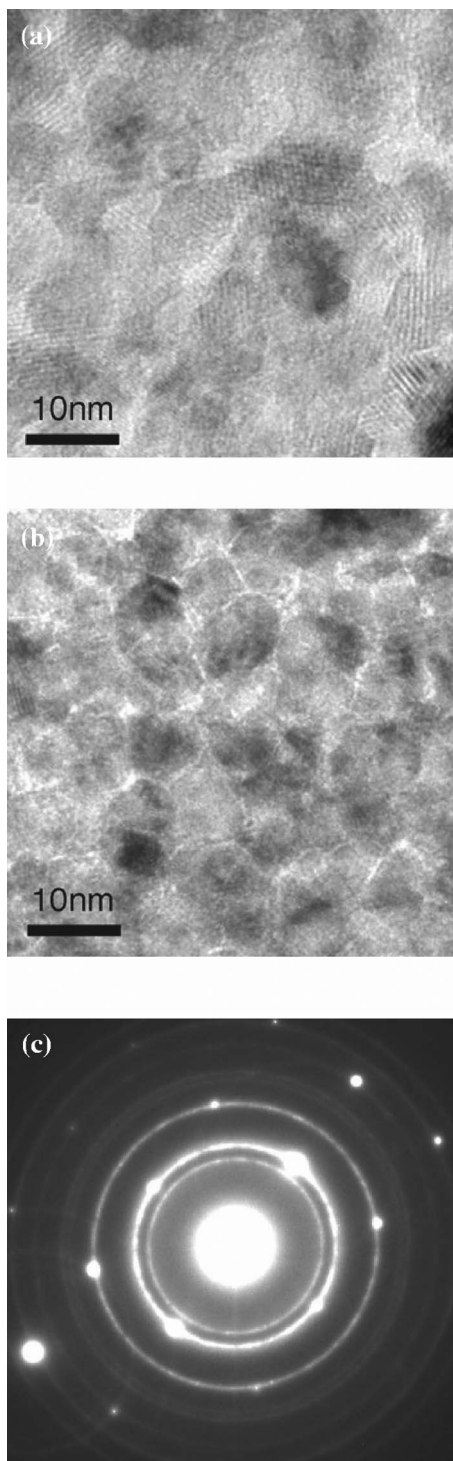


FIG. 2. TEM bright field image for (a) undoped and (b) 17% Co-doped Fe<sub>3</sub>O<sub>4</sub> film, and (c) SAED pattern for 17% Co-doped Fe<sub>3</sub>O<sub>4</sub> film.

## B. Transport properties

Fe<sub>3</sub>O<sub>4</sub> exhibits a characteristic order-disorder phase transition known as the Verwey transition at  $\sim 120$  K.<sup>17</sup> In order to investigate the effect of Co doping on the intrinsic metal-insulator Verwey transition in Fe<sub>3</sub>O<sub>4</sub>, we have analyzed the resistance of the undoped and Co-doped films as a function of temperature. As shown in Fig. 3, we observed that the undoped Fe<sub>3</sub>O<sub>4</sub> film exhibits an extremely smooth  $R$ - $T$  curve with a continuously changing slope, when compared with a

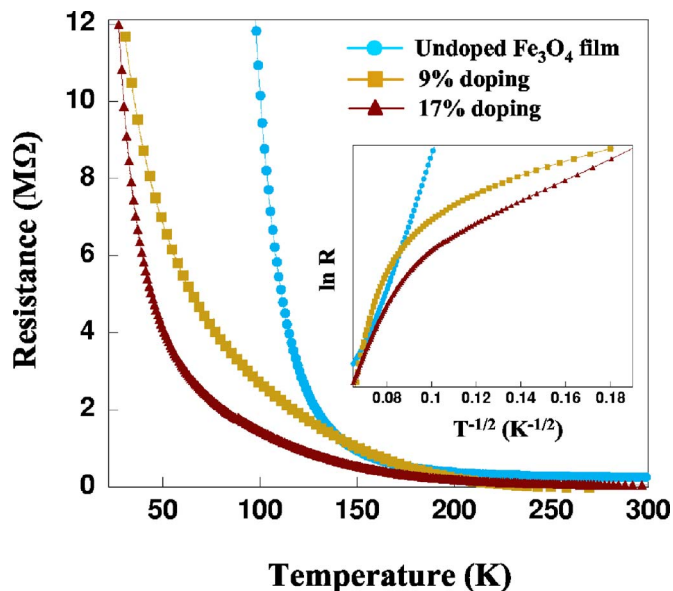


FIG. 3. (Color online) Resistance vs. temperature for Co-doped Fe<sub>3</sub>O<sub>4</sub> films as a function of Co doping concentration. Inset shows the corresponding logarithmic resistance as a function of  $T^{-1/2}$ .

sharp Verwey transition in which the resistance jumps by two orders of magnitude. This disappearance of the Verwey transition could be attributed to a variety of factors such as nonstoichiometric growth of Fe<sub>3</sub>O<sub>4</sub> due to room temperature deposition. It has been shown previously that an increased degree of nonstoichiometry in Fe<sub>3(1-δ)</sub>O<sub>4</sub> gives rise to a lowering and broadening of the Verwey transition, with the transition disappearing for  $\delta \sim 0.02$ .<sup>18-20</sup> The disappearance may also be due to substrate induced stress as a consequence of lattice mismatch between Fe<sub>3</sub>O<sub>4</sub> and MgO, which results in an in-plane expansion of the Fe<sub>3</sub>O<sub>4</sub> lattice accompanied by compression in the perpendicular direction.<sup>21</sup> It has also been suggested that the presence of a large density of grain boundaries<sup>22</sup> and small size of ferromagnetic domains or grains<sup>5</sup> may result in the disappearance of the Verwey transition in thin films of Fe<sub>3</sub>O<sub>4</sub>.

The Co-doped Fe<sub>3</sub>O<sub>4</sub> films also exhibit a smooth  $R$ - $T$  curve without any discontinuity. It has been suggested that Co<sup>2+</sup> ions usually replace the Fe<sup>2+</sup> ions at the octahedral  $B$  sites of the inverse spinel structure.<sup>23</sup> Mössbauer spectroscopy experiments have shown that for Co<sub>*x*</sub>Fe<sub>3-*x*</sub>O<sub>4</sub>, all Co<sup>2+</sup> ions are situated at the octahedral  $B$  sites.<sup>15,24,25</sup> As a result, the ionic distribution of the doped films can be expressed as (Fe<sup>3+</sup>)<sub>1</sub>{Co<sub>*x*</sub><sup>2+</sup>Fe<sub>1-*x*</sub><sup>2+</sup>Fe<sup>3+</sup>}O<sub>4</sub><sup>2-</sup>. Here ( ) denotes tetrahedral  $A$  lattice sites and { } denotes octahedral  $B$  lattice sites. The Verwey transition occurs at 120 K when the ordering energies of the Fe<sup>2+</sup> and Fe<sup>3+</sup> ions at the  $B$  sites overcome the thermal disturbance of these ions. The ordering accompanies the crystalline distortion which is caused by the difference of ionic radii of Fe<sup>2+</sup> and Fe<sup>3+</sup> ions. For the doped films however, the Co<sup>2+</sup> ions act as obstacles to the crystalline distortion.<sup>26</sup> In addition to the factors mentioned previously, this obstruction to the crystalline distortion could also contribute to the disappearance of the Verwey transition in the Co-doped films. The presence of a well defined grain boundary network in the undoped and Co-doped films, as revealed



from the TEM bright field images shown in Fig. 2, suggests that the transport properties of our films should be grain boundary controlled. In the inset of Fig. 3, we replot the temperature dependence of resistance as  $\ln R$  vs  $T^{1/2}$ . We observed that the resistance approximately follows the relation of  $R \sim \exp [(1/T)^{1/2}]$ . This linear relation between  $\ln R$  and  $T^{1/2}$  is expected for a granular system in which tunneling occurs through grain boundaries separating adjacent grains.<sup>22,27–29</sup>

### C. Magnetic properties

We have investigated the effect of Co doping on the magnetic properties of  $\text{Fe}_3\text{O}_4$ . Shown in Fig. 4 are the representative room temperature magnetization curves for the  $\text{Fe}_3\text{O}_4$  films measured as a function of Co doping concentration for magnetic fields applied parallel to the film surface. We observed low remanence and a coercive field of 140 Oe for the undoped  $\text{Fe}_3\text{O}_4$  film when magnetic field is applied parallel to the film plane. For the doped films, we observed an enhancement in coercivity of the in-plane magnetization curves from 323 to 478 Oe as the Co doping concentration is increased from 9% to 17%. This enhancement may be attributed to the increasing anisotropy in the doped films with increasing Co content. It should be noted that the  $\text{Co}^{2+}$  ion in the octahedral site of the inverse spinel structure contributes highly to the anisotropic character of our doped films. Further insight into the anisotropy contribution of  $\text{Co}^{2+}$  can be obtained from the “one-ion model” proposed by Slonczewski,<sup>30</sup> on the basis of orbital angular momentum of the ground state. The crystal electric field produces a degenerate ground state with an orbital angular momentum fixed parallel to a  $\langle 111 \rangle$  trigonal axis. The spin-orbit interaction tends to align the spin magnetic moment parallel to this trigonal axis, thus resulting in high anisotropy for the doped films.

We have also investigated the effect of temperature on the magnetic properties of Co-doped  $\text{Fe}_3\text{O}_4$  films. Figure 5 shows the dependence of coercivity on temperature for 9% and 17% Co-doped  $\text{Fe}_3\text{O}_4$  films. We can clearly see that for both doping concentrations, a large coercivity is observed at low temperatures, which decreases rapidly with increasing temperature. This suggests the occurrence of superparamagnetic effect in our Co-doped  $\text{Fe}_3\text{O}_4$  films. The magnetic anisotropy of the doped films also has strong temperature dependence. The anisotropy energy constants for Co substituted ferrites,  $K_1$  and  $K_2$ , are extremely sensitive to temperature and increase with decreasing temperature, thus resulting in higher anisotropy at low temperatures. This may be attributed to two main factors; namely, increase in both the exchange field due to neighboring spins and the effect of spin-orbit coupling, with decreasing temperature.<sup>31</sup>

### D. Magnetoresistance

We have investigated the MR properties of the undoped and Co-doped  $\text{Fe}_3\text{O}_4$  films in detail. Shown in Figs. 6(a) and 6(b) are the MR curves for the undoped  $\text{Fe}_3\text{O}_4$  films as a

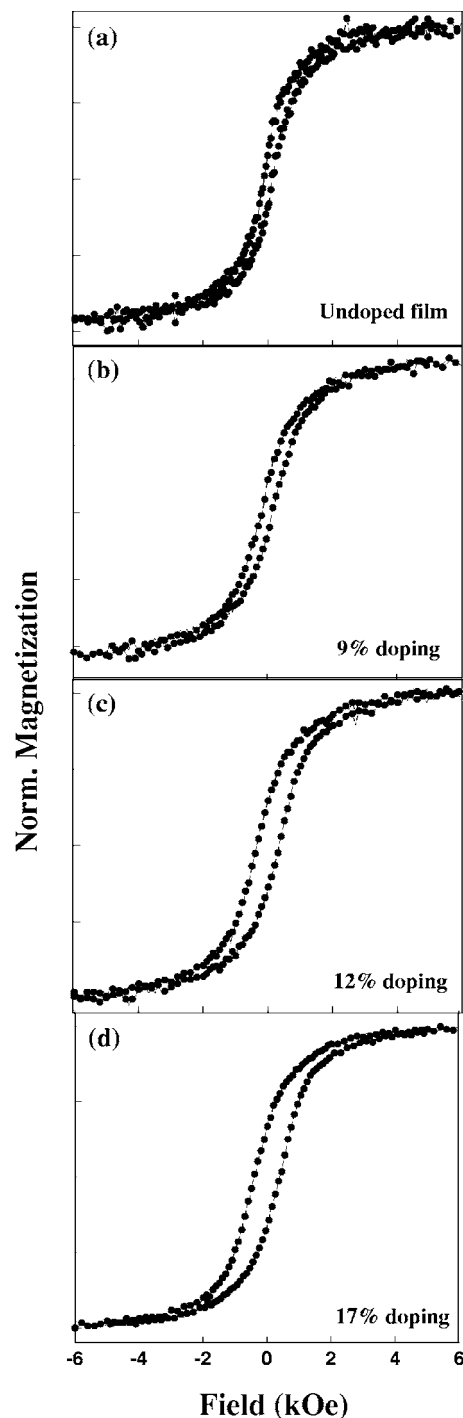


FIG. 4. Room temperature magnetization curves as a function of Co doping concentration for magnetic fields applied parallel to the film plane.

function of temperature, with magnetic field applied both parallel and perpendicular to the film plane. The MR ratio is defined as

$$\frac{\partial R}{R} \% = \frac{R_H - R_{H=0}}{R_{H=0}} \times 100. \quad (1)$$

We observed that for the undoped films, the in-plane MR ratio reaches its largest value of  $-4.5\%$  at 130 K, as shown in Fig. 6(a). MR decreases with increasing temperature and reaches a value of  $-3\%$  at room temperature. The corresponding out-of-plane MR has a maximum value of  $-3.8\%$

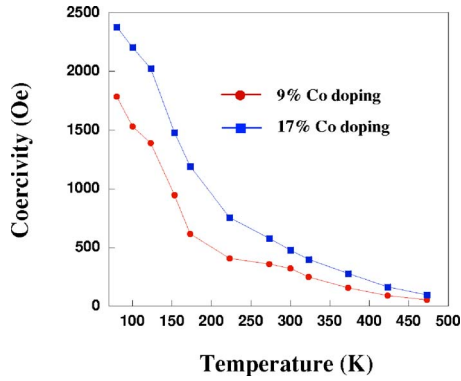


FIG. 5. (Color online) Coercivity as a function of temperature for 9% and 17% Co-doped  $\text{Fe}_3\text{O}_4$  films.

at 130 K and reduces  $-2\%$  at room temperature [Fig. 6(b)]. We can clearly see that the shape of the MR curves is independent of temperature and they show a very weak saturation trend for magnetic fields up to 3 T. We also observe that the preferential growth of our films as confirmed by the XRD results manifests itself in the form of totally distinct features for the in-plane and out-of-plane MR curves. The in-plane and out-of-plane MR curves show linear and quadratic behavior in the low magnetic field regime, whereas both vary linearly with magnetic field in the high field range.

Eerenstein *et al.*,<sup>32</sup> have suggested a model for spin-polarized tunneling of electrons across the AF interface between two antiphase domains to qualitatively explain the MR behavior in our undoped  $\text{Fe}_3\text{O}_4$  films. According to their model, the in-plane MR has been expressed as

$$\text{MR} \propto \frac{M_S H}{W_{\text{AF}}}. \quad (2)$$

For magnetic applied perpendicular to the plane of the film, the out-of-plane MR has been expressed as

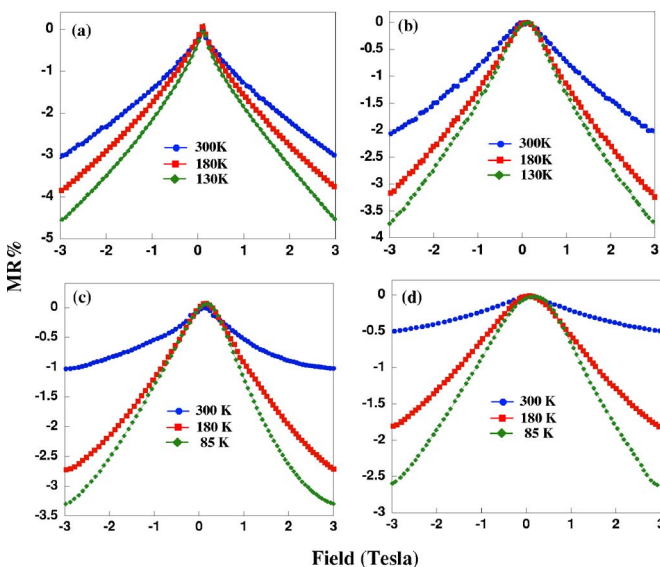


FIG. 6. (Color online) MR curves as a function of temperature for (a) undoped  $\text{Fe}_3\text{O}_4$  film with  $H$  parallel to the plane of the film, (b) undoped  $\text{Fe}_3\text{O}_4$  film with  $H$  perpendicular to the plane of the film, (c) 17% Co-doped  $\text{Fe}_3\text{O}_4$  film with  $H$  parallel to the plane of the film, and (d) 17% Co-doped  $\text{Fe}_3\text{O}_4$  film with  $H$  perpendicular to the plane of the film.

$$H < H_{\text{ah}} \rightarrow \text{MR} \propto \frac{(M_S H)^2}{4K W_{\text{AF}}}, \quad (3)$$

$$H > H_{\text{an}} \rightarrow \text{MR} \propto \frac{M_S H - K}{W_{\text{AF}}}, \quad (4)$$

where  $W_{\text{AF}} = A_{\text{AF}}^2 / A_{\text{F}} d^2$ ,  $A_{\text{AF}}$  and  $A_{\text{F}}$  are exchange stiffness constants,  $d$  is the distance between two neighboring spin chains along the boundary,  $H_{\text{an}}$  is the uniaxial anisotropy field, and  $K$  accounts for the uniaxial anisotropy energy. According to Eq. (2), the in-plane MR should increase linearly with magnetic field  $H$ . For magnetic fields applied perpendicular to the plane of the film, MR changes quadratically with field until it equals the anisotropy field and is approximately linear for higher magnetic fields. Our experimental observations for the undoped  $\text{Fe}_3\text{O}_4$  films are in good agreement with this model. This suggests that the grain boundaries in the undoped  $\text{Fe}_3\text{O}_4$  are AF coupled and have similar properties to antiphase boundaries (APB's).

Figures 6(c) and 6(d) shows the representative in-plane and out-of-plane MR curves for the 17% Co-doped  $\text{Fe}_3\text{O}_4$  films as a function of temperature. We observed a maximum in-plane MR of  $-3.4\%$  at 85 K which reduces further to  $-1\%$  at room temperature. For magnetic fields applied perpendicular to the plane of the film, a maximum MR of  $-2.55\%$  was observed at 85 K which decreases to  $-0.5\%$  at room temperature. The decrease in MR ratio for the Co-doped films when compared with undoped  $\text{Fe}_3\text{O}_4$  films may be attributed to a reduction in spin polarization of  $\text{Fe}_3\text{O}_4$  as a consequence of Co doping. We also observed that the in-plane MR curves do not change linearly with the applied field  $H$ . It should be noted that the model used to describe the MR behavior in undoped  $\text{Fe}_3\text{O}_4$  films only takes uniaxial anisotropy into account and ignores the small magnetocrystalline anisotropy in  $\text{Fe}_3\text{O}_4$ . Our Co-doped  $\text{Fe}_3\text{O}_4$  films, however, have a structure similar to polycrystalline Co ferrites and thus have strong cubic anisotropy. Consequently, linear in-plane MR behavior as predicted by the model is not observed in the Co-doped  $\text{Fe}_3\text{O}_4$  films. Preferential crystalline growth, however, results in different features for the in-plane and out-of-plane MR curves in the Co-doped  $\text{Fe}_3\text{O}_4$  films as well.

#### IV. CONCLUSIONS

In summary, we have investigated the structural, magnetic, and magnetotransport properties of Co-doped  $\text{Fe}_3\text{O}_4$  films fabricated at room temperature by cosputtering on MgO (100) substrates. XRD analysis suggests that the undoped and Co-doped  $\text{Fe}_3\text{O}_4$  films have a preferred crystalline orientation. Transmission electron microscopy confirms the presence of a well defined grain boundary network in the undoped and Co-doped films. We observed that the Verwey transition does not appear for our films. The magnetic and transport properties of  $\text{Fe}_3\text{O}_4$  are markedly sensitive to Co doping; the doped films exhibit highly anisotropic behavior which is confirmed further by temperature-dependent magnetization measurements. MR behavior in the undoped  $\text{Fe}_3\text{O}_4$  films shows linear magnetic field dependence for in-plane measurements and quadratic dependence for out of

plane measurements. These results are in agreement with the model of spin-dependent tunneling across AF coupled grain boundaries. For the Co-doped films, we observed that MR ratio decreases with increasing Co content and that there is a departure from linear field dependence for in-plane MR measurements.

## ACKNOWLEDGMENTS

This work was supported by the National University of Singapore (NUS) through Grant No. R263-000-283-112. One of the authors (D.T.) would like to thank NUS for his research scholarship.

- <sup>1</sup>G. Q. Gong, A. Gupta, G. Xiao, W. Qian, and V. P. Dravid, *Phys. Rev. B* **56**, 5096 (1997).
- <sup>2</sup>J. M. D. Coey, A. E. Berkowitz, L. Balcells, F. F. Putris, and F. T. Parker, *Appl. Phys. Lett.* **72**, 734 (1998).
- <sup>3</sup>S. B. Ogale, K. Ghosh, R. P. Sharma, R. L. Greene, R. Ramesh, and T. Venkatesan, *Phys. Rev. B* **57**, 7823 (1998).
- <sup>4</sup>S. Jain, A. O. Adeyeye, and D. Y. Dai, *J. Appl. Phys.* **95**, 7237 (2004).
- <sup>5</sup>D. Tripathy, A. O. Adeyeye, and C. B. Boothroyd, *J. Appl. Phys.* **99**, 08J105 (2006).
- <sup>6</sup>Z. Zhang and S. Sathpathy, *Phys. Rev. B* **44**, 13319 (1991).
- <sup>7</sup>Y. Yanase and K. Siratori, *J. Phys. Soc. Jpn.* **53**, 312 (1984).
- <sup>8</sup>F. Walz, *J. Phys.: Condens. Matter* **14**, R285 (2002).
- <sup>9</sup>J. M. Hastings and L. M. Corliss, *Phys. Rev.* **104**, 328 (1956).
- <sup>10</sup>M. Ishikawa, H. Tanaka, and T. Kawai, *Appl. Phys. Lett.* **86**, 222504 (2005).
- <sup>11</sup>C. T. Lie, P. C. Kuo, W. C. Hsu, I. J. Chang, and J. W. Chen, *J. Magn. Magn. Mater.* **239**, 160 (2002).
- <sup>12</sup>C. Y. Chou, P. C. Kou, Y. D. Yao, A. C. Sun, S. C. Chen, I. J. Chang, and J. W. Chen, *IEEE Trans. Magn.* **41**, 906 (2005).
- <sup>13</sup>R. F. Penoyer and L. R. Bickford, Jr., *Phys. Rev.* **108**, 271 (1957).
- <sup>14</sup>Y. Suzuki, R. B. van Dover, E. M. Gyorgy, J. M. Phillips, and R. J. Felder, *Phys. Rev. B* **53**, 14016 (1996).
- <sup>15</sup>M.-S. Lee, T.-Y. Kim, C.-S. Lee, J.-C. Park, Y. Kim, and D. Kim, *J. Magn. Magn. Mater.* **268**, 62 (2004).
- <sup>16</sup>Y. Peng, C. Park, J.-G. Zhu, R. M. White, and D. E. Laughlin, *J. Appl. Phys.* **95**, 6798 (2004).
- <sup>17</sup>E. J. W. Verwey, *Nature (London)* **144**, 327 (1939).
- <sup>18</sup>E. Lochner, K. A. Shaw, R. C. DiBari, W. Portwine, P. Stoyonov, S. D. Berry, and D. M. Lind, *IEEE Trans. Magn.* **30**, 4912 (1994).
- <sup>19</sup>Z. Kalol and J. M. Honig, *Phys. Rev. B* **40**, 9090 (1989).
- <sup>20</sup>R. Aragón, P. M. Gehring, and S. M. Shapiro, *Phys. Rev. Lett.* **70**, 1635 (1993).
- <sup>21</sup>D. T. Margulies, F. T. Parker, F. E. Spada, R. S. Goldman, J. Li, R. Sinclair, and A. E. Berkowitz, *Phys. Rev. B* **53**, 9175 (1996).
- <sup>22</sup>C. Park, Y. Peng, J. Zhu, D. E. Laughlin, and R. M. White, *J. Appl. Phys.* **97**, 10C303 (2005).
- <sup>23</sup>R. M. Bozorth, E. F. Tilden, and A. J. Williams, *Phys. Rev.* **99**, 1788 (1955).
- <sup>24</sup>H. Franke and M. Rosenberg, *J. Magn. Magn. Mater.* **4**, 186 (1977).
- <sup>25</sup>E. De Grave, R. Leyman, and R. Vanleerberghe, *Phys. Lett.* **97A**, 54 (1983).
- <sup>26</sup>R. Leyman and C. H. Iserentant, *Phys. Lett.* **97A**, 180 (1983).
- <sup>27</sup>P. Sheng, B. Abeles, and Y. Arie, *Phys. Rev. Lett.* **31**, 44 (1973).
- <sup>28</sup>H. Liu, E. Y. Jiang, H. L. Bai, R. K. Zheng, and X. X. Xiang, *Appl. Phys. Lett.* **83**, 3531 (2003).
- <sup>29</sup>H. Liu, E. Y. Jiang, H. L. Bai, R. K. Zheng, and X. X. Xiang, *J. Phys. D* **36**, 2950 (2003).
- <sup>30</sup>J. C. Slonczewski, *Phys. Rev.* **110**, 1341 (1958).
- <sup>31</sup>A. B. van Groenou, P. F. Bongers, and A. L. Stuyts, *Mater. Sci. Eng.* **3**, 317 (1968).
- <sup>32</sup>W. Eerenstein, T. T. M. Palstra, S. S. Saxena, and T. Hibma, *Phys. Rev. Lett.* **88**, 247204 (2002).